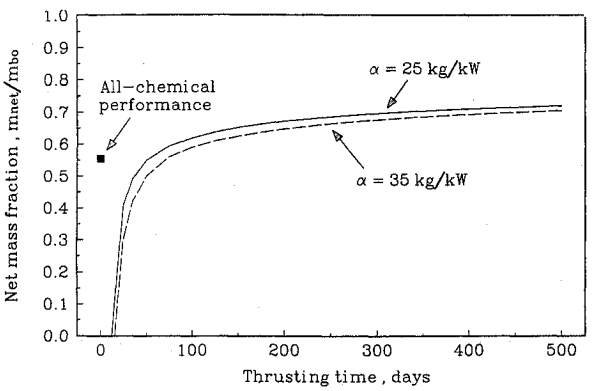

Fig. 2 Optimal net mass fraction.

rise in performance until the transfer time reaches about 75 days. The performance curves level off after about 150 days and approach asymptotic payload fractions of about 0.71 and 0.72 for $\alpha = 35$ and 25 kg/kW, respectively.

A summary of six representative maximum-net-mass solutions for $\alpha = 35$ kg/kW is presented in Table 1. The optimal P, I_{sp}, LOI altitude and inclination, low-thrust capture and escape transfer times, and payload fraction are shown in this table for a range of total transfer time. The optimal translunar injection trajectory results in a nearly polar orbit at LOI for all transfer times. Therefore, very little plane change is performed by the electric stage from LOI to polar LLO. Also, a direct chemical orbit insertion into polar LLO is optimal until the total transfer time is increased past 100 days.

Conclusions

A combined vehicle and mission optimization problem has been formulated and solved for a lunar–interplanetary mission using combined chemical and electric propulsion stages. The complex problem is solved by uncoupling the short-duration chemical insertion translunar phase from the long-duration electric propulsion phases, and the result is a very efficient, robust approach. Several optimal vehicle–mission combinations have been obtained for a range of transfer times from 16 to 500 days. A combined chemical–electric propulsion mission can provide an additional 15% payload capability compared to the corresponding all-chemical mission.

Acknowledgments

This research was funded by NASA Lewis Research Center under Grant NAG3-1650. The author would like to thank Mark Hickman, Steve Oleson, Kurt Hack, Jeff George, and Glen Horvat for their suggestions and contributions to this research project.

References

[1]Burton, R. L., and Wassgren, C., "Time-Critical Low-Thrust Orbit Transfer Optimization," *Journal of Spacecraft and Rockets*, Vol. 29, No. 2, 1992, pp. 286–288.

[2]Oleson, S. R., "An Analytical Optimization of Electric Propulsion Orbit Transfer Vehicles," NASA CR-191129, May 1993.

[3]Oleson, S. R., "Influence of Power System Technology on Electric Propulsion Missions," AIAA Paper 94-4138-CP, Aug. 1994.

[4]Kluever, C. A., and Pierson, B. L., "Vehicle-and-Trajectory Optimization of Nuclear Electric Spacecraft for Lunar Missions," *Journal of Spacecraft and Rockets*, Vol. 32, No. 1, 1995, pp. 126–132.

[5]Gilland, J. H., "Mission and System Optimization of Nuclear Electric Propulsion Vehicles for Lunar and Mars Missions," NASA CR-189058, Dec. 1991.

[6]Palaszewski, B., "Lunar Missions Using Advanced Chemical Propulsion: System Design Issues," *Journal of Spacecraft and Rockets*, Vol. 31, No. 3, 1994, pp. 458–465.

[7]Anon., "Delta II Payload Planner's Guide," McDonnell Douglas Astronautics, Doc. MDC-H3224C, Huntington Beach, CA, Oct. 1993.

[8]Pierson, B. L., "Sequential Quadratic Programming and Its Use in Optimal Control Model Comparisons," *Optimal Control Theory and Economic Analysis 3*, North-Holland, Amsterdam, 1988, pp. 175–193.

[9]Szebehely, V. G., *Theory of Orbits, the Restricted Problem of Three Bodies*, 1st ed., Academic Press, New York, 1967, pp. 7–21.

[10]Edelbaum, T. N., "Propulsion Requirements for Controllable Satellites," *ARS Journal*, Vol. 31, No. 8, 1961, pp. 1079–1089.

[11]Perkins, F. M., "Flight Mechanics of Low-Thrust Spacecraft," *Journal of the Aerospace Sciences*, Vol. 26, No. 5, 1959, pp. 291–297.

J. A. Martin
Associate Editor

Integrated Aerodynamic and Propulsive Flowfields of a Generic Hypersonic Space Plane

Ganesh Wadawadigi* and John C. Tannehill†
Iowa State University, Ames, Iowa 50011
and
Scott L. Lawrence‡ and Thomas A. Edwards§
NASA Ames Research Center, Moffett Field, California 94035

Introduction

A TYPICAL hypersonic space plane is envisioned to be an air-breathing vehicle equipped with a supersonic combustion ramjet (scramjet) engine with hydrogen as its fuel. One of the most important design aspects of the hypersonic space plane is the propulsion-airframe integration. The advantages of such a design in providing increased efficiencies have been well established. The high-Mach-number flight conditions for hypersonic space planes produce strong shocks in the external flowfield and lead to chemical reactions in the air surrounding the vehicle. This, coupled with the complicated combustion processes occurring in the scramjet, makes ground testing of such configurations extremely difficult and expensive. Thus, computational fluid dynamics (CFD) plays an important role in the analysis of the external as well as the internal flowfields of such configurations.

In the present paper, tip-to-tail flowfield calculations of the integrated aerodynamic and propulsive flowfields of the Test Technology Demonstrator[1] (TTD), shown in Fig. 1, have been performed. The TTD has an integrated propulsion airframe geometry which is typical of hypersonic space planes. The flow calculations are performed using an upwind parabolized Navier-Stokes (UPS) code. Two test cases are considered. The first one corresponds to a power-

Presented as Paper 94-0633 at the AIAA 32nd Aerospace Sciences Meeting, Reno, NV, Jan. 10–13, 1994; received Jan. 25, 1994; revision received April 12, 1994; accepted for publication April 13, 1994.

*Graduate Research Assistant, Department of Aerospace Engineering and Engineering Mechanics; currently Research Associate, Center for Hypersonic Research, University of Texas at Arlington, Arlington, TX 76019. Member AIAA.

†Manager, Computational Fluid Dynamics Center and Professor, Department of Aerospace Engineering and Engineering Mechanics. Fellow AIAA.

‡Research Scientist, Computational Aerosciences Branch. Member AIAA.

§Chief, Aerothermodynamics Branch. Senior Member AIAA.

Fig. 1 Test technology demonstrator (TTD) geometry.

off condition, where the fluid medium is assumed to be air in chemical nonequilibrium. The second one is a power-on condition, where the amount of hydrogen fuel injected at the throat of the scramjet results in stoichiometric conditions.

Numerical Approach

The UPS code was originally developed by Lawrence et al.[2] for perfect-gas flows. This three-dimensional (3-D) code solves the parabolized Navier-Stokes (PNS) equations in generalized coordinates. The parabolic-hyperbolic nature of these equations allows one to space-march the solution. The fluid-dynamic equations are integrated using a finite-volume, upwind, TVD scheme based on Roe's approximate Riemann solver.[3] The algorithm is second-order accurate in the crossflow plane and first-order accurate in the streamwise marching direction.

The UPS code has been extended to permit equilibrium and nonequilibrium airflow computations by Tannehill et al.[4] and Buelow et al.,[5] respectively. In addition, the UPS code has recently been enhanced to permit the calculation of internal flows with hydrogen-air chemistry by Wadawadigi et al.[6] For chemically reacting flows, the species continuity equations are solved in addition to the fluid-dynamic equations using a loosely coupled, upwind, finite-volume formulation. The air chemistry model[7] involves six species plus electrons (O_2, O, N, NO, NO^+, N_2, e^-) and seven reactions. The hydrogen-air chemistry model[8] consists of nine species (H, H_2O, OH, O, NO, N, H_2, O_2, N_2) and eleven reactions. Further details on the governing equations, chemistry models, thermodynamic and transport properties, and numerical algorithm can be found in Refs. 2 and 4–6. The UPS code has been rigorously tested by comparing results with other codes and experimental results for a wide range of flow conditions.[2,4–6,9–11]

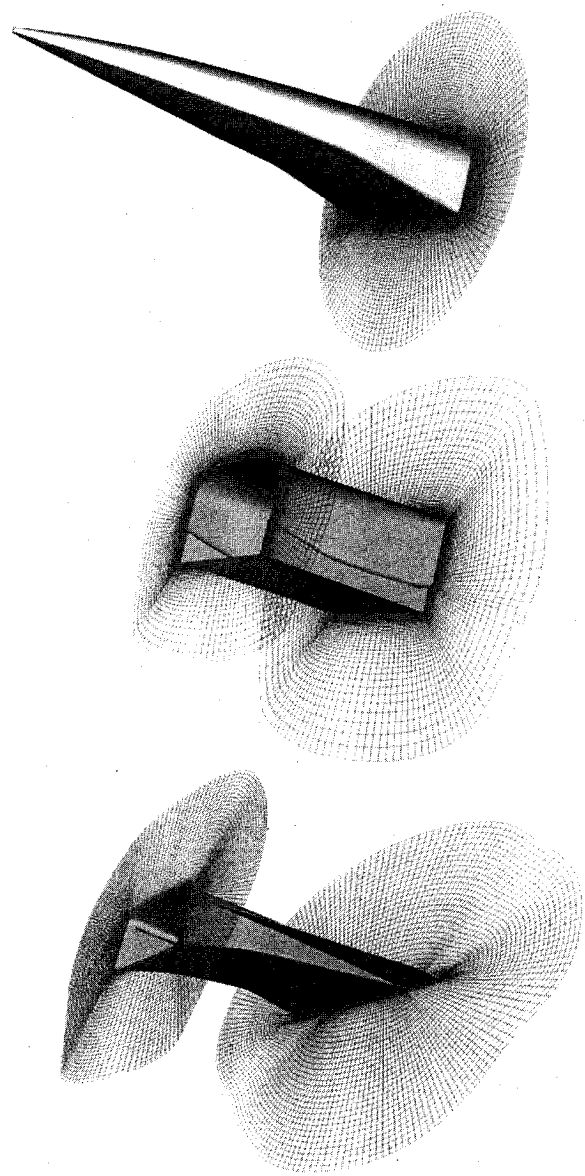

Fig. 2 TTD grids: forebody, midsection, aftbody.

Results

The freestream conditions for the present calculations correspond to an altitude of 30.5 km (100,000 ft), a Mach number (M_∞) of 10.05, and a Reynolds number (Re_∞) of $3.51 \times 10^6/M$. The freestream temperature is 227 K, and the wall temperature is held constant at 1000 K. The 3-D exterior grid for the TTD configuration consists of three zones (forebody, midsection, aftbody) as shown in Fig. 2. The grid sizes ($K \times L$) in each crossflow plane for the three zones are 65×65, 75×50, and 85×50, respectively, where K is in the crossflow direction and L is in the normal direction. The interior grid size for the scramjet engine in each crossflow plane is 40×82. Due to the symmetry of the configuration, the calculations are performed on one-half the cross section only. The air surrounding the TTD configuration is assumed to be in chemical nonequilibrium. Also, the algebraic turbulence model of Baldwin and Lomax, modified by Hung et al.,[12] is used.

The starting solution at the nose is obtained by using a conical stepback procedure.[13] The stepback procedure took 1200 steps to converge, producing a well-defined bow shock at the nose. With this starting solution two test cases were computed, one with power off and one with power on. The total computation time for the power-off case was 2 h 9 min on a Cray Y-MP.

To simulate the power-on condition, a stoichiometric amount of H_2 fuel is injected across the crossflow plane at the throat of the scramjet. The fuel is added at a static temperature of 2000 K. For simplicity, the velocity vector of the added fuel is taken to be the same as the local air flow. Also, to assist in the ignition process, a small amount of free radicals (H atoms) is added along with the fuel to enhance the chain-branching reactions. This was found necessary because of the simplified geometry of the scramjet engine used in this study. The mass and enthalpy are adjusted to account for the addition of the fuel and free radicals. As the freestream flow conditions are chosen to be the same as that for the power-off calculation; the forebody and the external flow over the midsection remain the same. The total tip-to-tail computation time for the power-on case was 2 h 38 min on a Cray Y-MP.

The Mach contours in crossflow planes along the length of the body are compared for the power-off and power-on cases in Fig. 3. As can be seen, the chosen freestream conditions result in the bow shock striking the cowl plate of the scramjet engine. This shock-on-lip condition provides an optimum operating condition. It is interesting to compare the shock structures in the aftbody region for the two cases. In the power-on case, due to the high temperature and pressure of the combustion products, the exhaust from the scramjet is underexpanded and thus is expanding through the external nozzle region. This results in the shock (on the underside) being pushed outward. Also, it can be observed that the bottom portion of the shock is much stronger in the power-on case than in the power-off case. Additional results can be found in Ref. 14.

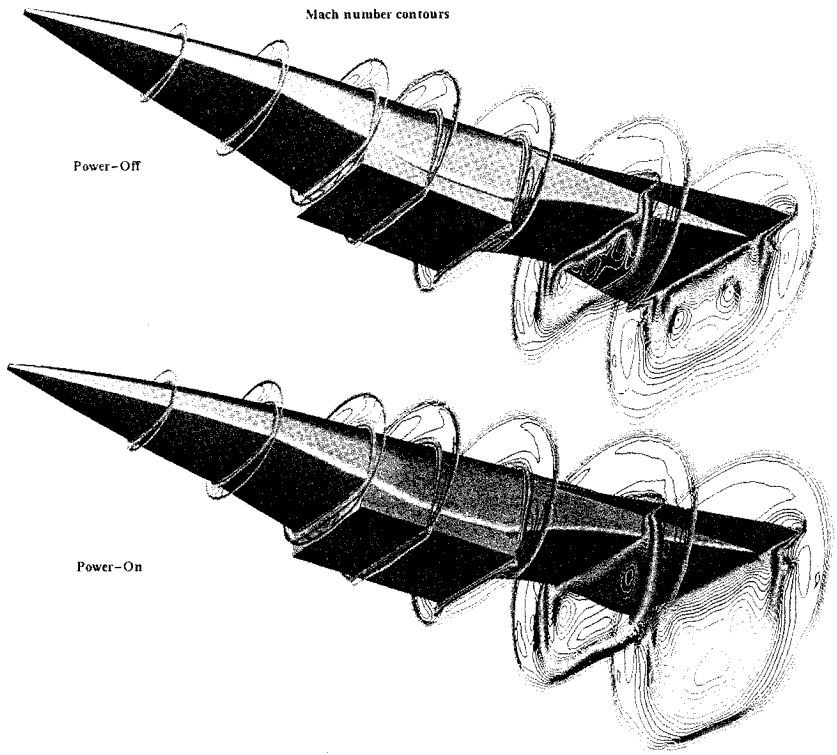

Fig. 3 Comparison of Mach contours in various crossflow planes along the length of the TTD configuration for the power-off and power-on calculations.

Concluding Remarks

In recent years the UPS code has been modified and enhanced to make it capable of solving more complex vehicle flowfields. In this study, the various capabilities of the UPS code have been demonstrated by computing the complete tip-to-tail flowfield of the TTD, a generic hypersonic vehicle geometry. Included in these calculations are the integrated aerodynamic and propulsive flowfields. Substantial savings in computing time and storage have been achieved by using the parabolized Navier-Stokes equations instead of the unsteady Navier-Stokes equations.

Acknowledgment

This work was supported by NASA Ames Research Center under Grant NAG 2-776.

References

[1]Huebner, L. D., and Haynes, D. A., "Computational TTD Forebody Redesign and Flow Characterization with Experimental Verification," NASP TT-1013, expected publication May 1994.

[2]Lawrence, S. L., Chaussee, D. S., and Tannehill, J. C., "Application of an Upwind Algorithm to the Three-Dimensional Parabolized Navier–Stokes Equations," *AIAA Journal*, Vol. 28, No. 6, 1990, pp. 971–972.

[3]Roe, P. L., "Approximate Riemann Solvers, Parameter Vectors, and Difference Schemes," *Journal of Computational Physics*, Vol. 43, 1983, pp. 357–372.

[4]Tannehill, J. C., Buelow, P. E., Ievalts, J. O., and Lawrence, S. L., "Three-Dimensional Upwind Parabolized Navier–Stokes Code for Real Gas Flows," *Journal of Spacecraft and Rockets,* Vol. 27, No. 2, 1990, pp. 150–159.

[5]Buelow, P. E., Tannehill, J. C., Ievalts, J. O., and Lawrence, S. L., "A Three-Dimensional, Upwind, Parabolized Navier–Stokes Code for Chemically Reacting Flows," *Journal of Thermophysics and Heat Transfer,* Vol. 5, No. 3, 1991, pp. 274–283.

[6]Wadawadigi, G., Tannehill, J. C., Buelow, P. E., and Lawrence, S. L., "Three-Dimensional Upwind Parabolized Navier–Stokes Code for Supersonic Combustion Flowfields," *Journal of Thermophysics and Heat Transfer,* Vol. 7, No. 4, 1993, pp. 661–667.

[7]Blottner, F. G., Johnson, M., and Ellis, M. "Chemically Reacting Viscous Flow Program for Multi-Component Gas Mixtures," Sandia Laboratories, Albuquerque, NM, Report SC-RR-70-754, Dec. 1971.

[8]Oldenberg, R., Chinitz, W., Friedman, M., Jaffe, R., Jachimowski, C., Rabinowitz, M., and Schott, G., "Hypersonic Combustion Kinetics: Status Report of the Rate Constant Committee, NASP High Speed Propulsion Technology Team," NASP TM-1107, May 1990.

[9]Buelow, P. E., Ievalts, J. O., and Tannehill, J. C., "Comparison of Three-Dimensional Nonequilibrium PNS Codes," AIAA Paper 90-1572, June 1990.

[10]Lockman, W. K., Lawrence, S. L., and Cleary, J. W., "Flow Over an All-Body Hypersonic Aircraft: Experiment and Computation," *Journal of Spacecraft and Rockets,* Vol. 29, No. 1, 1992, pp. 7–15.

[11]Wadawadigi, G., Tannehill, J. C., Edwards, T. A., Lawrence, S. L., and Molvik, G. A., "Application of a Two-Equation Turbulence Model to Supersonic Combustion Flowfields," AIAA Paper 94-0705, Jan. 1994.

[12]Hung, C.-M., and Buning, P. G., "Simulation of Blunt-Fin-Induced Shock-Wave and Turbulent Boundary-Layer Interaction," *Journal of Fluid Mechanics*, Vol. 154, 1985, pp. 163–185.

[13]Lawrence, S. L., "Application of Space-Marching Methods to Hypersonic Forebody Flow Fields," AIAA Paper 92-5030, Dec. 1992.

[14]Wadawadigi, G., Tannehill, J. C., Lawrence, S. L., and Edwards, T. A., "Three-Dimensional Computation of the Integrated Aerodynamic and Propulsive Flowfields of a Generic Hypersonic Space Plane," AIAA Paper 94-0633, Jan. 1994.

K. J. Weilmuenster
Associate Editor